

# A study in the mechanical milling of alumina powder

Caroline B. Reid<sup>a</sup>, Jennifer S. Forrester<sup>b,\*</sup>, Heather J. Goodshaw<sup>b</sup>,  
Erich H. Kisi<sup>b</sup>, Gregg J. Suaning<sup>b,c</sup>

<sup>a</sup> *Department of Medical Physics, University College London, Malet Place Engineering Building, London, United Kingdom*

<sup>b</sup> *School of Engineering, University of Newcastle, Callaghan, 2308 New South Wales, Australia*

<sup>c</sup> *Graduate School of Biomedical Engineering, University of New South Wales, Sydney, 2052 New South Wales, Australia*

Received 8 March 2007; received in revised form 21 March 2007; accepted 2 May 2007

Available online 2 June 2007

## Abstract

The mechanical milling of alumina in order to reduce grain sizes to  $\leq 100$  nm has been proposed as a means of reducing sintering temperatures and improving pressureless sintered density, particularly as a means of allowing co-firing with metallic components for biomedical implants. There is a persistent problem with contamination from the milling media, usually hardened steel which can be only partially alleviated by acid leaching. We have explored the use of alternative milling media with a view to reducing the levels of contamination. Alumina powders were milled with hardened steel, tungsten carbide, alumina and zirconia milling media under identical conditions of ball mass:powder mass ratio 10:1 and target milling times of 32 h. All of the milling media were found to cause unacceptable levels of contamination. Zirconia media gave the lowest contamination (3–4%) and in some circumstances, the addition of a small amount of zirconia may lead to increased toughness without loss of biocompatibility.

© 2007 Elsevier Ltd and Techna Group S.r.l. All rights reserved.

**Keywords:** D.  $\text{Al}_2\text{O}_3$ ; Alumina; Mechanical milling; Milling media; Contamination

## 1. Introduction

Alumina powder is a versatile material which can be sintered into useful ceramics with applications in many industries. It is a known biocompatible material useful in medical devices such as surgical implants [1,2]. Alumina is normally sintered into dense ceramic components at around 1700 °C [3]. Medical devices such as the cochlear implant make use of alumina as the feedthrough matrix through which electrical signals to the body are transmitted (e.g. see [4]). The high temperatures required to sinter alumina into dense ceramics dictate that metallic components co-fired within devices possess a very high melting temperature.

Potential applications may expand significantly if the required sintering temperature could be decreased. To this end, it is known that dopants such as  $\text{MnO}_2$ ,  $\text{TiO}_2$ ,  $\text{MgO}$  and several other elemental oxides and nitrides can reduce the sintering temperature required to obtain full densification of alumina [5,6].

In the processing of ceramic materials, very small grain sizes generally increase the surface to volume ratio of the particulate, and promote sintering through increased diffusion. This can lead to a reduction in the sintering temperature. Mechanical milling is known to decrease grain sizes to the level of some tens of nanometres, and therefore is potentially useful in the processing of alumina when co-fired with low ( $\leq 1700$  °C) melting point metals such as Pt for use in biomedical devices.

The milling vial and balls used to grind materials during the mechanical milling process are commonly referred to as the “milling media”. Large attrition mills are normally constructed from hardened steel because of the low cost compared to other materials. High energy milling vials on the laboratory scale are small (normally a few centimetres in diameter), and may be constructed from many different materials including hardened steel. The milling balls are normally made to match the vial. Commercially available high energy milling media include carbide-based materials such as WC and SiC, and the ceramics  $\text{ZrO}_2$  and  $\text{Al}_2\text{O}_3$ .

A major problem is contamination from the milling media due to the high hardness of alumina. In published work on the milling of alumina, this aspect is often ignored. For example, in

\* Corresponding author. Tel.: +61 2 4921 6117; fax: +61 2 4921 7050.

E-mail address: [Jenny.Forrester@newcastle.edu.au](mailto:Jenny.Forrester@newcastle.edu.au) (J.S. Forrester).

a study where alumina powder was milled using hardened steel and tungsten carbide milling media [7], there was no mention of contamination, even though in the published X-ray diffraction patterns significant contamination was clearly visible. The importance of this contamination depends on the application. The commonly used hardened steel vial and balls generally result in significant iron contamination [8]. This can be unimportant, or in some cases it might even be useful. In the manufacture of some artificial gems, such as sapphire, colour centres are introduced by percentage level additions of powders such as Fe and Cr oxides [9]. Such additions can be made using controlled mechanical milling. In biomedical applications however, contamination can be a limiting factor for use, as contaminants are a potential source of biological degradation of the component. There have been some claims that Fe contamination can be removed with HCl treatment [8] however traces of Fe remain [10].

In this work, the milling of alumina powder was studied using various milling media, to compare the degree of contamination from each, and to examine the effectiveness of these in reducing the crystallite size of the powders. Rietveld refinements using X-ray diffraction patterns collected from milled powders was used to estimate crystallite sizes, and also to provide a quantitative estimate of the amount of contamination from each of the milling media. Scanning electron microscopy was used to observe the morphology of the milled samples.

## 2. Experimental

The powder used was commercially available alumina (99.9%, Aldrich, Australia). As some of the milling media are also alumina, for the purpose of this work, the processed powder is referred to as “alumina” and the milling media are referred to as “Al<sub>2</sub>O<sub>3</sub>” (similar nomenclature is used for zirconia, ZrO<sub>2</sub>, etc.). All powders were dry-milled in air using a SPEX 8000 high energy mixer/mill. The initial milling ball diameter in all tests was 10 mm. Experiments were conducted under the conditions shown in Table 1.

Milling times were determined through initial tests on samples using the selected milling media, with the objective of finding a common milling time by which all the samples could be compared. These tests led to a selected mass charge ratio of 10:1 (ratio of grinding balls to powder, CR), and a milling time of 32 h. These conditions were chosen because this allows sufficient milled powder (approximately 1–2 g) to allow for the collection of XRD patterns and also to produce samples for electron microscopy. Test 4 and 5 runs were terminated early

due to visible damage to the milling media. In particular, a longer milling time would have ultimately resulted in the complete disintegration of the balls. The combination of balls in Test 5 was conducted as a result of the previous tests.

Approximately 30% of each milled powder was soaked in boiling HCl solution, which has been shown to dissolve much of the Fe contamination in powder milled using Fe milling media [8]. The procedure is based on Fe dissolution resulting in a FeCl<sub>3</sub> solution. This solution is subsequently decanted off to leave a clean alumina powder. In our previous work [10], using this procedure a reduction in Fe was indeed achieved, however XRF analysis indicated that up to 2% of Fe contamination remained following the cleaning procedure.

X-ray diffraction (XRD) patterns from the milled products were collected in the range 10–90° 2θ with 0.04° step size, using a Philips 1710 powder diffractometer with Cu Kα radiation and fitted with a graphite monochromator. XRD patterns were also collected from the powders after soaking in HCL solution to determine the extent of contamination reduction.

Rietveld refinements based upon XRD patterns was used to investigate aspects of milling such as phase proportions, crystallite sizes, changes in lattice parameters of the alumina, and micro-strains. Collection times were varied according to sample perfection. Refinements were performed using the computer program LHPM [11]. The crystallite size component of the peak shape broadening was estimated here using the Sec θ dependence of particle size broadening and an assumed Lorentzian peak shape [12].

X-ray fluorescence (XRF) analyses were conducted using a Spectro X-Lab 2000 spectrometer using samples absorbed into a lithium borate flux.

Secondary and back-scattered electron images were obtained using a Philips XL30 scanning electron microscope (SEM), operated at 15 kV. When required, elemental spectra were collected using an Oxford ISIS Si/(Li) energy dispersive spectroscopy (EDS) detector. Powders were prepared for SEM analysis by mounting in epoxy resin, and polishing to a 1 μm finish using diamond paste.

## 3. Results

XRD patterns recorded from milled powders are shown in Fig. 1. A control (unmilled) alumina powder is shown in Fig. 1(a) to comprise mostly α-alumina with the corundum structure and a very minor amount of β-alumina (~2%). XRF elemental analysis showed the absence of any significant contaminants. Additional diffraction peaks in other XRD patterns show that contamination occurs with *each* type of

Table 1  
Milling conditions for each of the tests

Test	Vial	Balls	Charge ratio (CR)	Time (h)
1	Hardened steel (Fe)	Hardened Fe	10:1	32
2	Tungsten carbide (WC)	WC	10:1	32
3	Partially stabilised zirconia (ZrO <sub>2</sub> )	Yttria stabilised tetragonal zirconia polycrystal (TZP)	10:1	32
4	Alumina (Al <sub>2</sub> O <sub>3</sub> )	Al <sub>2</sub> O <sub>3</sub>	10:1	4
5	Al <sub>2</sub> O <sub>3</sub>	TZP and Al <sub>2</sub> O <sub>3</sub>	10:1	4

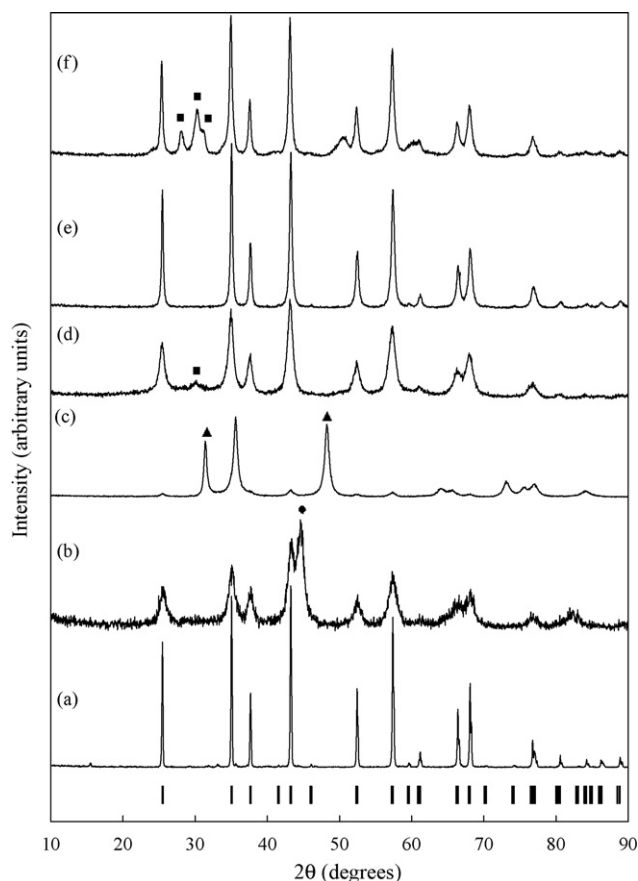


Fig. 1. XRD patterns from  $\text{Al}_2\text{O}_3$  powders using selected milling media (a) unmilled, (b) hardened Fe balls and vial (●, Fe contamination), (c) WC balls and vial (▲, WC contamination) (d)  $\text{ZrO}_2$  balls in an  $\text{ZrO}_2$  vial (■,  $\text{ZrO}_2$  contamination), (e)  $\text{Al}_2\text{O}_3$  balls and  $\text{Al}_2\text{O}_3$  vial, and (f)  $\text{Al}_2\text{O}_3$  vial and  $\text{Al}_2\text{O}_3$  and  $\text{ZrO}_2$  balls. The marker below the XRD patterns are the  $h k l$  markers for  $\alpha$ -alumina.

milling albeit to a different extent (apart from milling in alumina media).

Rietveld refinement results are shown in Tables 2 and 3. Table 2 shows the refined parameters for the alumina crystal structure in each sample such as the lattice parameters and crystallite size. An estimate of the amount of contamination from each milling medium in each sample is given in the phase proportions in Table 3. An example of a Rietveld fit is shown in Fig. 2.

The following were observed from the XRD patterns, the XRF analyses and the Rietveld refinements:

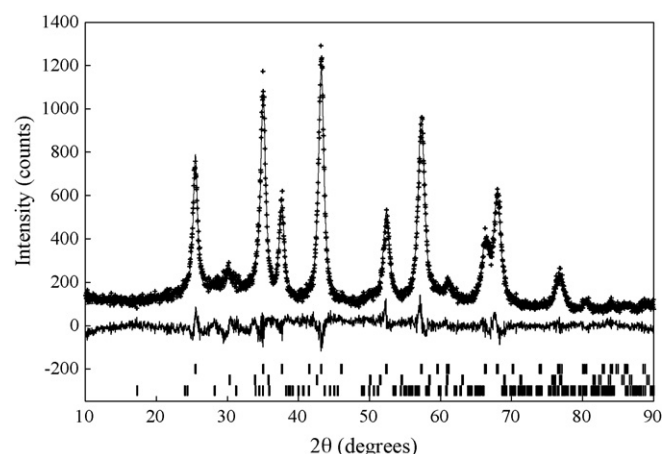


Fig. 2. Rietveld refinement of the XRD pattern of alumina milled for 32 h using  $\text{ZrO}_2$  milling media. (+) represents the experimental pattern, the solid line is the calculated pattern, and the line below is the difference pattern between the calculated and experimental patterns. Below this are the  $h k l$  markers for  $\alpha$ -alumina, tetragonal  $\text{ZrO}_2$  and monoclinic  $\text{ZrO}_2$  (from top to bottom).

**Test 1:** Milling with Fe balls and vial caused considerable Fe contamination in the alumina powder (Fig. 1(b)). The large diffraction peak of the Fe is evident at approximately  $45^\circ 2\theta$ . XRF analysis showed that in the alumina milled for 32 h there was approximately 16% Fe contamination, which caused the sample to appear black instead of the characteristic white of alumina. The result was similar in the XRD analysis (approximately 11% of crystalline Fe indicated). XRF analysis showed that this contamination was reduced to approximately 2% following the HCl cleaning procedure.

**Test 2:** After milling the alumina powder using WC media, the powder was again black in colour, an indication of significant contamination. The XRD pattern (Fig. 1(c)) shows that the contribution of WC to the pattern is quite high. Phase quantification (Table 2) estimates this value at 35%. In this regard, these media are considered unsuccessful. The degree of contamination suggests that even though the crystallite size achieved is comparable to hardened Fe milling balls (approximately 100 Å in each, see Table 1), the level of contamination is much higher. XRF analysis showed that this contamination was unchanged following the HCl cleaning procedure. In fact no change was shown in the contamination levels of any of the powders apart from that milled in Fe milling media.

**Test 3:** This was the most successful test according to XRF analyses to determine the degree of contamination. These

Table 2  
Refined lattice parameters, Lorentzian FWHM, Gaussian FWHM ( $U$ ), crystallite size (nm) and  $R_B$  factors

Milling time (h), charge ratio	Milling media	$a$ (Å)	$c$ (Å)	Lorentzian FWHM	Gaussian FWHM ( $U$ )	Crystallite size (nm)	$R_B$ ( $\text{Al}_2\text{O}_3$ )
0	—	4.7589(2) <sup>a</sup>	12.9912(5)	0.053(1)	0.030(2)	426.7	4.62
32, CR 10:1	Fe balls, Fe vial	4.771(2)	13.033(8)	0.68(6)	1.1(3)	10.6	2.85
32, CR 10:1	WC balls, WC vial	4.775(3)	13.04(2)	0.69(3)	1.03(2)	9.8	3.33
32, CR 10:1	$\text{ZrO}_2$ balls, $\text{ZrO}_2$ vial	4.7775(5)	13.048(2)	0.69(2)	1.081(4)	12.6	2.43
4, CR 10:1	$\text{Al}_2\text{O}_3$ balls, $\text{Al}_2\text{O}_3$ vial	4.7597(3)	12.994(1)	0.283(2)	1.14(1)	31.2	2.68
4, CR 10:1	$\text{Al}_2\text{O}_3$ and $\text{ZrO}_2$ balls, $\text{Al}_2\text{O}_3$ vial	4.7775(4)	13.042(2)	0.312(5)	0.961(6)	28.3	3.72

<sup>a</sup> The number in parentheses is the estimated standard deviation determined during the Rietveld analyses.



Table 3

Phase proportions obtained from the Rietveld refinements

Milling time (h), charge ratio	Milling media	Wt.% alumina	Wt.% impurity	Wt.% impurity
0	–	100	–	–
32, CR 10:1	Fe balls, Fe vial	89.0	11.0 Fe	–
32, CR 10:1	WC balls, WC vial	65.3	34.7	–
32, CR 10:1	ZrO <sub>2</sub> balls, ZrO <sub>2</sub> vial	96.4	1.5 <i>t</i> -ZrO <sub>2</sub>	2.2 <i>m</i> -ZrO <sub>2</sub>
4, CR 10:1	Al <sub>2</sub> O <sub>3</sub> balls, Al <sub>2</sub> O <sub>3</sub> vial	100	–	–
4, CR 10:1	Al <sub>2</sub> O <sub>3</sub> and ZrO <sub>2</sub> balls, Al <sub>2</sub> O <sub>3</sub> vial	87.4	7.6 <i>t</i> -ZrO <sub>2</sub>	5.0 <i>m</i> -ZrO <sub>2</sub>

analyses showed that after milling, there was 3–4% contamination from the ZrO<sub>2</sub> media (Fig. 1(d)) following milling. The average crystallite size gained from Rietveld refinement shows that the size is comparable to tests 1 and 2 above.

**Test 4:** Al<sub>2</sub>O<sub>3</sub> balls with an Al<sub>2</sub>O<sub>3</sub> vial were by comparison an unsuccessful combination. At the start of milling, the charge ratio was 10:1. After milling for 4 h, the total ball weight had

decreased by 27%. However, the powder weight increased by 438%. Of this increase 91% can be attributed to an increase in powder mass by the breakdown of the balls, leaving 9% of the powder increase to the degradation of the walls of the milling vial. Of 100% powder at the end of the test, 62.5% was from the balls, 22.8% was from the vial wall, and only 14.7% was the starting powder. In addition, the crystallite size given in Table 2

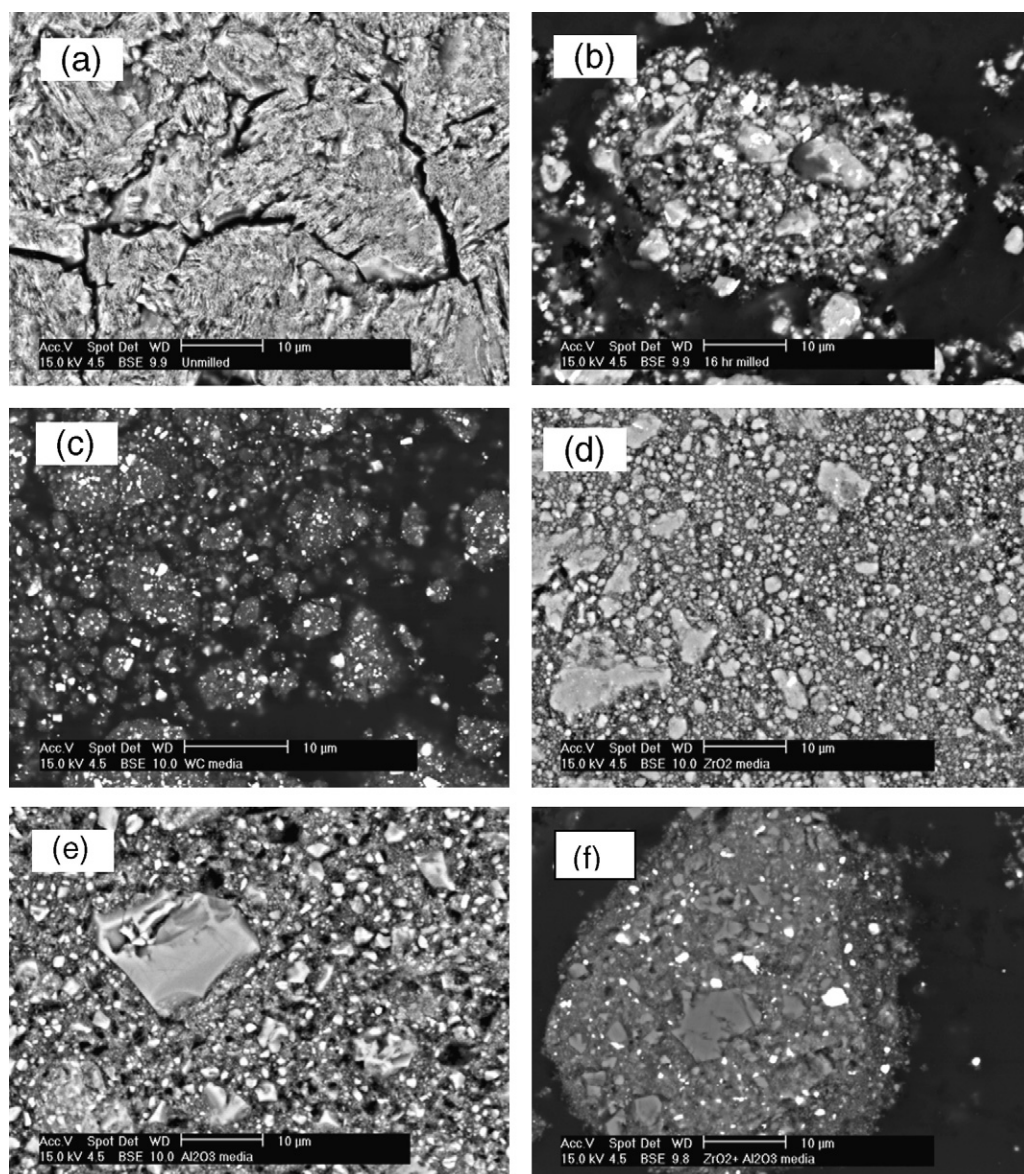


Fig. 3. Back-scattered electron images from (a) an unmilled alumina particle; and from milled samples (b) in hardened steel milling media, (c) in WC, (d) in an ZrO<sub>2</sub> vial using ZrO<sub>2</sub> balls, (e) in an Al<sub>2</sub>O<sub>3</sub> vial and balls, and (f) in an Al<sub>2</sub>O<sub>3</sub> vial using ZrO<sub>2</sub> and Al<sub>2</sub>O<sub>3</sub> balls.

is approximately 300 Å, significantly greater than in tests 1–3. This can also be seen by the narrower peak widths of this sample in Fig. 1(e).

**Test 5:** This procedure performed poorly in regard to contamination. A combination of milling balls increased degradation in both types of balls. There was a combined decrease in milling ball weight of 49% after only 4 h. The XRD pattern (Fig. 1(f)) shows significant diffraction peaks at around 30° 2θ that were identified as belonging to tetragonal and monoclinic zirconia. Subsequent Rietveld analyses (Table 2) show that approximately 12.5% of this contamination can be attributed to ZrO<sub>2</sub>.

SEM back-scattered electron micrographs of each sample are shown in Fig. 3. The alumina particles are darker and the contaminants are lighter. Contamination is most obvious in Fig. 3(b), (c) and (f): Fe, WC and a combination of Al<sub>2</sub>O<sub>3</sub> and ZrO<sub>2</sub> balls. Less contamination is evident in Fig. 3(d) (ZrO<sub>2</sub> milling media). In Fig. 3(e), the sample milled in Al<sub>2</sub>O<sub>3</sub> milling media, the lack of contrast indicates little contamination; however a notable feature of this sample is that there are very large particles. It is believed that these large particles are the remains of either the vial or balls that have been eroded during the milling process.

The agglomerate size and largest particles can also be observed in Fig. 3, and is comparable from Fe, WC and ZrO<sub>2</sub> media. However, the samples milled with Al<sub>2</sub>O<sub>3</sub>, and Al<sub>2</sub>O<sub>3</sub> and ZrO<sub>2</sub> media (Fig. 3(e) and (f)) show that the larger particles in both instances are substantially bigger. It should be noted that the particle sizes determined by XRD refer to the mean coherent scattering domain and will be dominated by the smaller sizes.

#### 4. Discussion

It would be useful to decrease the sintering temperature of alumina while still allowing dense ceramic components to be produced. In addition to the obvious reduction in production costs, it would allow co-firing of alumina with other materials such as lower melting point metals, and open up potential new applications. One such application is in biomedical devices where a ceramic must be co-fired with a metal, such as a platinum electrode. An avenue for reducing the sintering temperature is particle size reduction. Mechanical milling is a known method of reducing the particle size (e.g. see [13]).

The Rietveld refinement results of alumina milled in ZrO<sub>2</sub> media (Table 3) indicate there is much less contamination compared to the other milling media tested (approximately 3–4%). This is important for several reasons:

- a small amount of contamination will have less impact on the alumina properties.
- ZrO<sub>2</sub> is not soluble in alumina and the resultant powder when sintered should have no colour alteration (of value in marketing products).
- the degree of wear of the milling balls and vial is significantly less thereby prolonging the lifetime of the milling media.

- ZrO<sub>2</sub> is known to have better mechanical properties than alumina (e.g. higher fracture toughness and tensile strength). The addition of dispersed ZrO<sub>2</sub> particles could reinforce the alumina after sintering. Zhan et al. [14] found a threefold increase in the strength of alumina with 3-mol% zirconia added over pure alumina.

HCl is known to dissolve the Fe following the milling of alumina [8]. Attempts to use HCl to clean other samples were unsuccessful. The XRD patterns collected following soaking in HCl were identical to those reported previously [10] as was the colour of the powders. There may be an avenue for cleaning other contaminants such as ZrO<sub>2</sub> from the milled alumina; however in the case of ZrO<sub>2</sub> it is likely that a solvent for ZrO<sub>2</sub> will also dissolve Al<sub>2</sub>O<sub>3</sub>. The application of milled alumina to biomedical applications may indeed be assisted by the addition of a small percentage of ZrO<sub>2</sub>. Piconi and Maccauro have reviewed zirconia as a biomaterial [15]. Zirconia was first researched as a biomaterial about 40 years ago, and is now an accepted material used in the manufacture of hip joint heads. More than 300 000 have been implanted with only two failures.

The use of Al<sub>2</sub>O<sub>3</sub> milling media (Test 4) as a means to eliminate contamination manifests its own problems. The high hardness of the milling media and powder, and the low fracture toughness of alumina, means that the balls and vial are eroded quickly. It is difficult to obtain the nano-scale grain sizes that this type of milling is aimed at, because large particles of alumina are continually being added to the processed alumina powder from the vial and balls.

We have found that sieving the powders after milling eliminates the large particles of alumina contributed by the milling media. However, EDS spectra have shown that contaminants from the alumina vial that have been milled to a small grain size (thus becoming part of the sieved alumina powder) has small amounts of elements present such as ZrO<sub>2</sub> (presumably used in the production of the vial). Indeed, milling alumina in Al<sub>2</sub>O<sub>3</sub> milling media has problems akin to the other media.

From the perspective of hardness, the only media capable of milling alumina without the problem of contamination may well be sintered diamond and diamond-like substances (e.g. *c*-BN). Anything softer than alumina will be eroded by the alumina powder. Whether any advantage can be gained from the use of ultra-hard media remains to be seen as the wear resistance of hard materials is governed also by the fracture toughness.

#### 5. Conclusions

From this work we can conclude that all of the commonly available high energy milling media lead to unacceptable levels of contamination when milling alumina powders. Furthermore, acid leaching does not remove all of the contamination because of the tightly agglomerated nature of the milled powders. The least contamination occurs when using ZrO<sub>2</sub> media and in some circumstances, this contamination may lead to a beneficial effect on toughness.

## Acknowledgements

The authors thank the Research Grants Committee of the University of Newcastle for funding this research. We thank Mr David Phelan for assistance with the electron microscopy.

## References

- [1] A.H. De Aza, J. Chevalier, G. Fantozzi, M. Schehl, R. Torrecillas, *Biomaterials* 23 (2002) 937–945.
- [2] J. Li, Y. Liu, L. Hermansson, R. Söremark, *Clin. Mater.* 12 (1993) 197–201.
- [3] W.C. Johnson, R.L. Coble, *J. Am. Ceram. Soc.* 61 (1978) 110–114.
- [4] C.H. Chouard, P. Pialoux, *Bull. Acad. Natl. Med.* 179 (1995) 549–555.
- [5] I.V. Cutler, C. Bradshaw, C.J. Christensen, E.P. Hyatt, *J. Am. Ceram. Soc.* 40 (1957) 134–139.
- [6] S. Rossignal, C. Kappenstein, *Int. J. Inorg. Mater.* 3 (2001) 51–58.
- [7] Y. Wang, C. Suryanarayana, L. An, *J. Am. Ceram. Soc.* 88 (2005) 780–783.
- [8] G.R. Karagedov, N.Z. Lyakhov, *Nanostruct. Mater.* 11 (1999) 559–572.
- [9] M. Kayama, J. Kuwano, *J. Cryst. Growth* 193 (1998) 648–655.
- [10] H.J. Goodshaw, J.S. Forrester, G.J. Suaning, E.H. Kisi, *J. Mater. Sci.* (2006).
- [11] C.J. Howard, B.A. Hunter, A Computer Program for Rietveld Analysis of X-ray and Neutron Diffraction Patterns, ANSTO Lucas Heights Research Laboratories, 1997.
- [12] H.P. Klug, L.E. Alexander, *X-ray Diffraction Procedures for Polycrystalline and Amorphous Materials*, 2nd ed., John Wiley and Sons, New York, 1974, p. 662.
- [13] B.B. Bokhonov, L.G. Konstanchuk, V.V. Boldyrev, *Mater. Res. Bull.* 30 (1995) 1277–1284.
- [14] G.D. Zhan, J. Kuntz, J. Wan, J. Garay, A.K. Mukherjee, *J. Am. Ceram. Soc.* 86 (2003) 200–202.
- [15] C. Piconi, G. Maccauro, *Biomaterials* 20 (1999) 1–25.